http://dx.doi.org/10.5012/bkcs.2012.33.7.2407

DFT Study of the [Cu-Angiotensin II]$^{2+}$ Complex Structure

Bo-Ra Kim and Ho-Tae Kim*

Department of Applied Chemistry, Kumoh National Institute of Technology, Gumi 730-701, Korea
**E-mail: hotaekim@kumoh.ac.kr*
Received March 10, 2012, Accepted April 2, 2012

Key Words : Blood pressure, Angiotensin II, Metal-peptide complex, [Metal-Ang II]$^{2+}$ complex, DFT calculation

Angiotensin II (Ang II, an octapeptide hormone: Asp1-Arg2-Val3-Tyr4-Ile5-His6-Pro7-Phe8) has been studied for several decades in investigations of the structure-dependent activity of the renin-angiotensin blood pressure regulation system.[1-4] Metal ion influences on the biological activity of Ang II have also been investigated.[5-14] Blood pressure was observed to increase as a result of the influence of Li, Na, Mg, and Ca ions on the renin-angiotensin system. Thus, it was proposed that the alkali (or alkaline-earth) metal ions induced conformational changes in Ang II that led to a conformational structure more suitable for the biological activity of Ang II. However, the Cu ion was observed to reduce blood pressure in a study performed by separate research group.[12-14] A few different positive ion complexes [Cu-Ang II]$^{n+}$ have been studied. The Cu binding sites of the [Cu-Ang II]$^{1+}$ complex were suggested to have a Cu-NNNN geometry in the ATCUN (Amino Terminal Cu(II) and Ni(II)) complex.[15-16] However, the Cu binding sites in the [Cu-Ang II]$^{2+}$ complex were suggested to be the oxygen atoms of the carbonyl functional groups.[10,17] The structure of Ang II has been reported to be S-shaped according to the results of an NMR experiment.[18] This S-shaped structure has two potential metal ion binding pockets (Fig. 1).

Different patterns of interaction between metal ions (Mg, Cu, and Ni) and Ang II have been reported as a result of the different fragmentation patterns obtained in an electrospray ionization mass spectrometry (ESI-MS) experiment.[19] The Mg ion was reported to choose the 'B' binding pocket (Ile5-His6-Pro7-Phe8) in the [Mg-Ang II]$^{2+}$ complex. However, Cu and Ni ions were reported to choose the 'A' binding pocket (Asp1-Arg2-Val3-Tyr4) in the [Cu (or Ni)-Ang II]$^{2+}$ complexes. The metal ion binding sites of Ang II were reported to be the amide oxygen atoms instead of the deprotonated peptide nitrogen atoms (N^-). In the gas phase, the ligand affinities of alkaline earth metal and transition metal ions have been reported based on the results of a collision-induced dissociation (CID) experiment using ESI-MS measurement.[20-22]

The present paper focuses on the interaction between a Cu ion and the 'A' pocket of the Ang II molecule. The interaction between a Cu ion and the carbonyl oxygen atoms of Ang II is studied in terms of optimized structures obtained from *ab initio* calculations. The *ab initio* calculations were performed to determine both the optimized structures and the SCF energies of the [Cu-Ang II]$^{2+}$ complex. These optimized structures and their SCF energies are reported.

Methods

Ab initio calculations were performed with LANL2DZ basis sets to determine the optimized structures and SCF energies. Density functional theory (DFT) at the B3LYP level was carried out using the Gaussian03 series program.[23] DFT was chosen because DFT is less computationally demanding than other computational methods but has similar accuracy in ground-state energy calculations.[24] The energies of the optimized gas-phase structures in water solution were calculated using single-point energy calculations at the B3LYP/LANL2DZ level with the UAKS cavities using conductor-like polarizable continuum model (CPCM).[25,26] The vibrational frequencies were also calculated at the B3LYP level to confirm that the optimized geometries correspond to true minima on the potential energy surface. Zero-point energy corrections were not included in the energy calculations.

Results and Discussion

The two potential 'A' and 'B' binding pockets for a Cu ion in the [Cu-Ang II]$^{2+}$ complex are shown in the schematic diagram in Figure 1. The 'A' pocket was supposed to be a favorable Cu ion binding site based on ESI-MS experimental observations.[19] The schematics of four possible [Cu-Ang II]$^{2+}$ geometries (with the interactions between the Cu ion and the four or five ligand atoms of the Ang II 'A' binding pocket) for the geometry optimization are shown in Figure 2. Two four-coordination structures (complex 1 and complex 2) and two five-coordination structures (complex 3 and complex 4) were considered in the attempt to optimize the [Cu-Ang II]$^{2+}$ complex structure. The deprotonated peptide nitrogen atoms (N^-) were excluded as the Cu ion

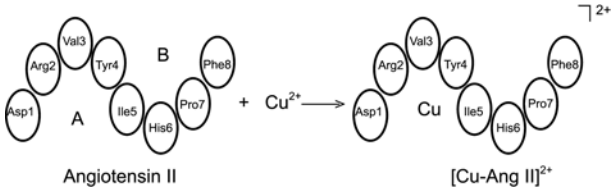

Figure 1. Schematic structures of Ang II and the [Cu-(Ang II)]$^{2+}$ complex.

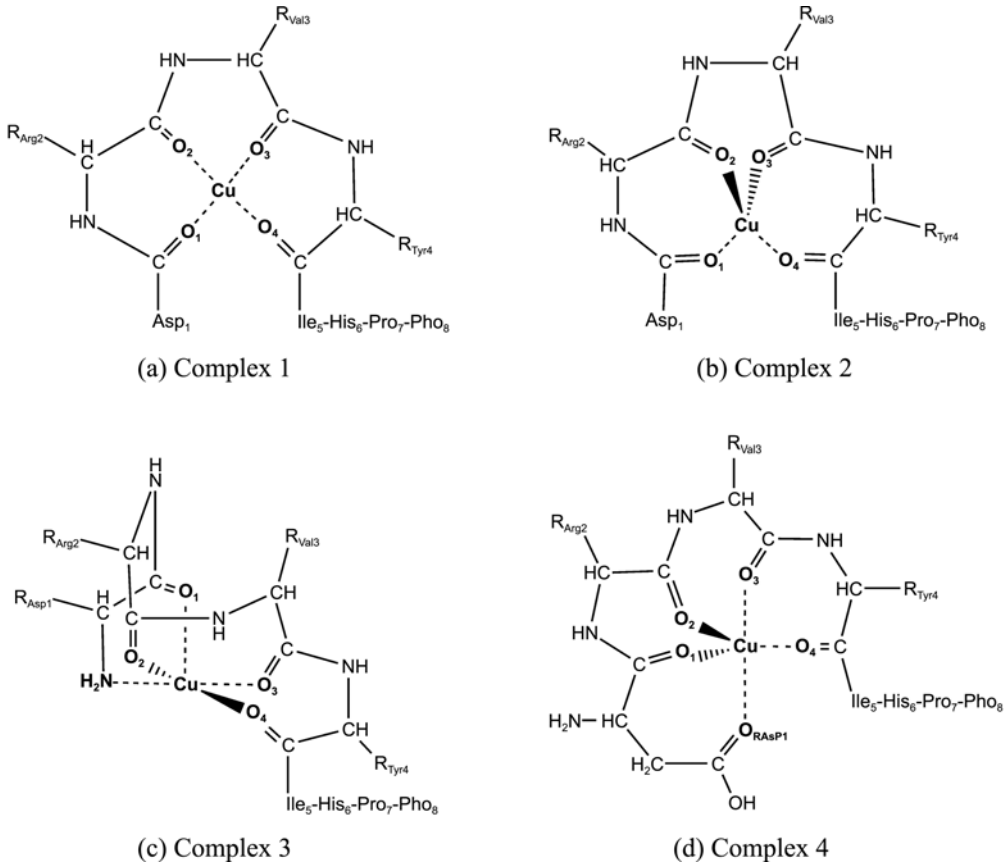

Figure 2. Schematic structures of the four starting $[Cu\text{-}(Ang\ II)]^{2+}$ complex geometries.

binding sites because of the positive 2+ charge state of the $[Cu\text{-}Ang\ II]^{2+}$ complex. Metal ions have been proposed to interact with peptide carbonyl oxygen atoms at pH values at which the peptide bond is not deprotonated.[10,17] The geometry optimization was performed while considering the double hydrogen bonds between the carboxyl group of Asp1 and the guanidyl group of Arg2 in the structures of complexes 1-3. However, complex 4 cannot have these double hydrogen bonds between Asp1 and Arg2, because the fifth ligand oxygen atom (O_{1R}) participates in the Cu-$O_{1R}O_1O_3O_4O_2$ coordination geometry (Fig. 2(d)).

Among the four-coordination structures, a square-planar geometry and a tetrahedral geometry were tested for the geometry optimization. The trial square-planar geometry is shown in Figure 2(a) as the complex 1 structure. In this trial square-planar geometry, four amide oxygen atoms ($O_1O_2O_3O_4$) are coordinated to a Cu ion in the same plane. However, in the optimized square-planar geometry shown in Figure 3(a), the five atoms (Cu ion, O_1, O_2, O_3, and O_4) of complex 1 are not located in the same plane. While the four atoms(Cu ion, O_1, O_3, and O_4) of complex 1 are located on the same plane (the observed Cu-O_1-O_3-O_4 dihedral angle, –2.8°, was almost zero in Table 1), the carbonyl oxygen atom of Arg2 (O_2) deviates from the Cu-O_1-O_3-O_4 plane in this optimized complex 1 structure. Bond distances, bond angles, and dihedral angles of the optimized square-planar geometry (complex 1) are listed in Table 1. The bond distances, bond angles and dihedral angles fall in the 1.916

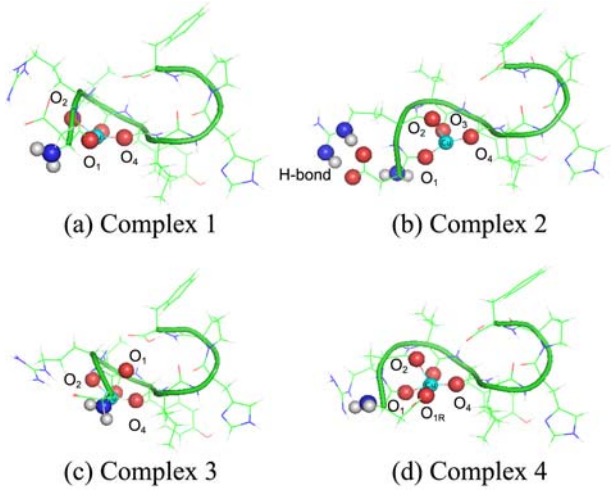

Figure 3. Five optimized structures of the $[Cu\text{-}(Ang\ II)]^{2+}$ complex from B3LYP/LANL2DZ calculations. The backbone atoms of 'B' binding pocket are shown in a paper plane. The N-terminal amine group is shown for emphasis. (Top view)

Å - 2.102 Å, 85.1° - 92.7° and –2.8° - (–24.1°) ranges, respectively. Comparing these with the ideal square-planar bond distance (equivalent bond distance), bond angle (90°), and dihedral angle (0°) in the metal-ligand complex, it seems that there is some geometric constraint in the optimized complex 1 geometry. This geometric constraint of complex 1 results in its unstable SCF energy in Table 2.

The relative SCF energies for complexes 1-4 are listed in

Table 1. Optimized geometric parameters of the [Cu-(Ang II)]$^{2+}$ complex from B3LYP/LANL2DZ calculations

	Bond distance (Å)				
	O_1-Cu	O_2-Cu	O_3-Cu	O_4-Cu	$N_t(O_{1R})$-Cu
complex 1	1.916	2.102	1.985	2.003	
complex 2	1.878	2.134	2.068	1.899	
complex 3	3.122	2.063	1.961	2.001	2.018
complex 4	1.998	2.252	1.983	1.941	2.064
	Bond angle (°)					
	O_1-Cu-O_2	O_2-Cu-O_3	O_3-Cu-O_4	O_1-Cu-O_4	O_1-Cu-O_{1R}	$N_t(O_{1R})$-Cu-O_2
complex 1	85.1	91.2	88.9	92.7		
complex 2	95.5	83.5	97.2	155.4		
complex 3	78.8	87.9	89.5	67.1		92.3
complex 4	83.0	81.1	94.3	164.5	88.3	95.1
	Dihedral angle (°)				
	O_1-O_2-O_3-O_4	Cu-O_1-O_3-O_4	N_t-O_2-O_3-O_4	N_t-O_3-O_4-Cu	O_{1R}-O_1-O_3-O_4
complex 1	−24.1	−2.8			
complex 3			−32.6	−8.2	
complex 4		−10.5			−12.6

Table 2 as the energy difference from the complex 1 and fall in a −29.2 to 5.4 kcal/mol range based on the gas-phase B3LYP/LANL2DZ calculations. The complex 4 geometry is calculated to be the most unstable geometry in the gas-phase [Cu-Ang II]$^{2+}$ complex because of the zero number of hydrogen bonds between Asp1 and Arg2. Among the three complexes with identical numbers of hydrogen bonds (complexes 1-3), the tetragonal-pyramidal complex 3 geometry (Cu-$N_tO_2O_3O_4O_1$) is supposed to be the most stable geometry based on the gas-phase SCF energy calculations. It is worth to note that the SCF energy of the tetrahedral complex 2 geometry is lower than that of the square-planar complex 1 geometry by 20.1 kcal/mol. The 20.1 kcal/mol stabilization energy of the tetrahedral complex 2 geometry is thought to originate from the relaxation of the geometric constraint in the square-planar complex 1 geometry. As mentioned before, the O_2 atom deviates from the Cu-O_1-O_3-O_4 plane in the optimized complex 1 structure (Fig. 3(a)). This deviation is thought to originate from the rigidity of the double hydrogen bonds between the carboxyl group of Asp1 and the guanidyl group of Arg2. It is supposed that the rigidity of these double hydrogen bonds is relaxed by the long tail-extension backbone structure of the 'A' pocket in Figure 3(b) and Figure 4(b). The rigidity of the double hydrogen bonds between Asp1 and Arg2 is a common characteristic of the structures of complexes 1-3.

In the complex 3 geometry optimization process, a fifth ligand (the N-terminal nitrogen atom, N_t) was added to the four-coordination (Cu-$O_1O_2O_3O_4$) geometry. The complex 3 structure (Cu-$N_tO_2O_3O_4O_1$) was optimized to a tetragonal-pyramidal geometry, as shown in Figure 3(c). The carbonyl oxygen atom of Asp1 (O_1) is located at the apex of the optimized tetragonal-pyramidal geometry. The O_1-Cu bond is supposed to be a weak bond because of its long bond distance (3.122 Å). The other four ligand atoms ($N_tO_2O_3O_4$) were optimized to a distorted square-planar geometry (the observed N_t-O_2-O_3-O_4 dihedral angle was −32.6°). The bond distances, bond angles, and dihedral angles of the tetragonal-pyramidal (Cu-$N_tO_2O_3O_4O_1$) geometry are listed in Table 1. The SCF energy of complex 3 is the lowest in the gas-phase SCF calculations. However, the energy of complex 2 is the lowest in the water solution SCF calculations (the CPCM-UAKS method was applied). The observed SCF energy difference between complex 2 and complex 3 was 2.4 kcal/mol. The optimized complex 2 structure is supposed to be a favorable structure in water solution because of the less congested geometry in the Cu-$O_1O_2O_3O_4$ vicinity (Fig. 3(b)). The congestion of the Cu-$N_tO_2O_3O_4O_1$ vicinity in the optimized complex 3 structure results in a protrusion of the Cu-N_t-O_2-O_3-O_4 square-planar plane from the peptide

Table 2. Calculated energies of the four optimized [Cu---Ang II]$^{2+}$ complexes in gas-phase and in aqueous solution

	SCF Energy (gas-phase)		SCF Energy (water solution)	
	B3LYP/LANL2DZ (hartree)	Δ^a (kcal/mol)	CPCM-UAKS (hartree)	Δ^a (kcal/mol)
complex 1	−3757.954632	0.0	−3758.206676	0.0
complex 2	−3757.986635	−20.1	−3758.242699	−22.6
complex 3	−3758.001198	−29.2	−3758.238861	−20.2
complex 4	−3757.946021	5.4	−3758.215044	−5.3

[a]Energy difference = Energy (Complex n) − Energy (Complex 1)

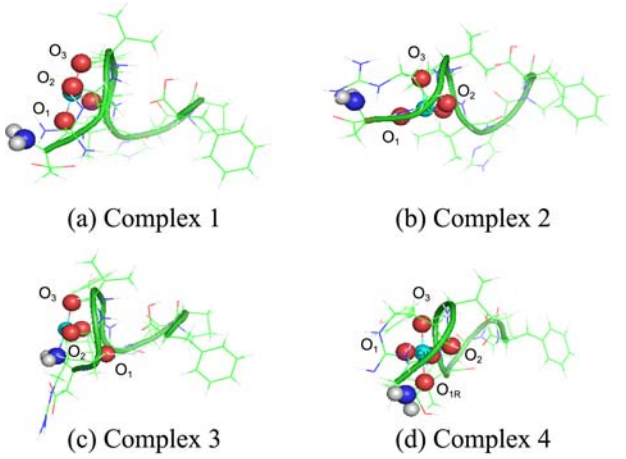

Figure 4. Five optimized structures of the $[Cu\text{-}(Ang\ II)]^{2+}$ complex from B3LYP/LANL2DZ calculations. The N-terminal amine group is shown for emphasis. (Side view)

backbone axis (Fig. 4(c)). This protrusion of the square-planar plane from the peptide backbone axis is also observed in the optimized complex 1 structure (Fig. 4(a)).

The trigonal-bipyramidal complex 4 geometry was tested as one of the five-coordination geometries in the geometry optimization. Two oxygen atoms (O_3 and O_{1R}) are located at the two apexes of the trigonal-bipyramidal starting geometry of complex 4 (Fig. 2(d)). However, the trigonal-bipyramidal complex 4 geometry was optimized to an almost tetragonal-pyramidal geometry with O_2 at the apex and four oxygen atoms (O_{1R}, O_1, O_3, and O_4) in the square-planar plane (Fig. 3(d)). The trial O_1-Cu-O_4 angle (120°) in the trigonal-bipyramidal complex 4 geometry was optimized to 164.5° (Table 1). This expansion of the O_1-Cu-O_4 angle modified the original trigonal-bipyramidal geometry to an almost tetragonal-pyramidal geometry with an O_{1R}-O_1-O_3-O_4 dihedral angle of −12.6°. The other bond angles fall in the 81.1°-95.1° range in the complex 4 structure. The SCF energies in water solution show that the complex 4 geometry, which is the most unstable in the gas-phase, is no longer the most unstable geometry in water solution. The SCF energy difference between complex 4 and complex 1 was observed to be −5.3 kcal/mol in water solution.

Conclusions

In the interaction between a Cu ion and the 'A' pocket moiety of the Ang II molecule, both the tetrahedral complex 2 geometry and the tetragonal-pyramidal complex 3 geometry appear to be favorable from the SCF energy viewpoint. The complex 3 structure is calculated to be the most stable structure in the gas-phase $[Cu\text{-}Ang\ II]^{2+}$ complex. This five-coordination complex 3 structure results in a protrusion of the Cu-N_t-O_2-O_3-O_4 square-planar plane from the peptide backbone axis. The four-coordination complex 2 structure is calculated to be the most favorable structure among the complex 1-4 geometries in water solution because of the less congested geometry of the long tail-extension backbone structure of the 'A' pocket.

Acknowledgments. This paper was supported by Research Fund, Kumoh National Institute of Technology.

References

1. Garcia, K. C.; Ronco, P. M.; Verroust, P. J.; Brunger, A. T.; Amzel, L. M. *Science* **1992**, *257*, 502.
2. Gasparo, M. D.; Catt, K. J.; Inagami, T.; Wright, J. W.; Unger, T. *Pharmacol. Rev.* **2000**, *52*, 415.
3. Deraët, M.; Rihakova, L.; Boucard, A.; Pèrodin, J.; Sauvé, S.; Mathieu, A. P.; Guillemette, G.; Leduc, R.; Lavigne, P.; Escher, E. *Can. J. Physiol. Pharmacol*. **2002**, *80*, 418.
4. Boucard, A. A.; Wilkes, B. C.; Laporte, S. A.; Escher, E.; Guillemette, G.; Leduc, R. *Biochem.* **2000**, *39*, 9662.
5. Schaechtelin, G.; Walter, R.; Salomon, H.; Jelínek, J.; Karen, P.; Cort, J. H. *Mol. Pharmacol.* **1974**, *10*, 57.
6. Gaggelli, E.; D'Amelio, N.; Gaggelli, N.; Valensin, D.; Maccotta, A.; Valensin, G. *Res. Devel. Inorg. Chem*. **2000**, *2*, 131.
7. Bridgewater, J. D.; Lim, J.; Vachet, R. W. *Anal. Chem.* **2006**, *78*, 2432.
8. Amelio, N. D.; Gaggelli, E.; Gaggelli, N.; Mancini, F.; Molteni, E.; Valensin, D.; Valensin, G. *J. Inorg. Biochem.* **2003**, *95*, 225.
9. Gokhale, N. H.; Cowan, J. A. *Chem. Commun*. **2005**, 5916.
10. Hu, P.; Loo, J. A. *J. Am. Chem. Soc.* **1995**, *117*, 11314.
11. Reverend, B. D.; Liman, F.; Livera, C.; Pettit, L. D.; Pyburn, S.; Kozlowski, H. J. *Chem. Soc. Dalton Trans.* **1988**, 887.
12. Moore, R. J.; Klevay, L. M. *Nutr. Res.* **1988**, *8*, 489.
13. Wu, B. N.; Medeiros, D. M.; Lin, K.-N.; Thorne, B. M. *Nutr. Res*. **1984**, *4*, 305.
14. Fields, M.; Ferretti, R. J.; Smith, J. C., Jr.; Reiser, S. *Life Sci.* **1983**, *34*, 763.
15. Camerman, N.; Camerman, A.; Sarkar, B. *Can. J. Chem.* **1976**, *54*, 1309.
16. Laussac, J.-P.; Sarkar, B. *Can. J. Chem.* **1980**, *58*, 2055.
17. Liu, D.; Seuthe, A. B.; Ehrler, O. T.; Zhang, X.; Wyttenbach, T.; Hsu, J. F.; Bowers, M. T. *J. Am. Chem. Soc.* **2005**, *127*, 2024.
18. Spyroulias, G. A.; Nikolakopoulou, P.; Tzakos, A.; Gerothanassis, I. P.; Magafa, V.; Manessi-Zoupa, E.; Cordopatis, P. *Eur. J. Biochem.* **2003**, *270*, 2163.
19. Kim, J.-Y.; Kim, H.-T. *Bull. Korean Chem. Soc.* **2010**, *31*, 1377.
20. Hu, P.; Gross, M. L. *J. Am. Chem. Soc.* **1992**, *114*, 9153.
21. Hu, P.; Gross, M. L. *J. Am. Chem. Soc.* **1993**, *115*, 8821.
22. Kim, B.-R.; Kim, H.-T. *Bull. Korean Chem. Soc.* **2007**, *28*, 840.
23. Frisch, M. J.; Tucks, G. W.; Schlegel, H. B.; Scuseria, G. E.; Robb, M. A.; Cheeseman, J. R.; Montgomery, J. A.; Vreven, T.; Kudin, K. N.; Burant, J. C.; Millam, J. M.; Iyengar, S. S.; Tomasi, J.; Barone, V.; Mennucci, B.; Cossi, M.; Scalmani, G.; Rega, N.; Petersson, G. A.; Nakatsuji, H.; Hada, M.; Ehara, M.; Toyota, K.; Fukuda, R.; Hasegawa, J.; Ishida, M.; Nakajima, T.; Honda, Y.; Kitao, O.; Nakai, H.; Klene, M.; Li, X.; Knox, J. E.; Hratchian, H. P.; Cross, J. B.; Bakken, V.; Adamo, C.; Jaramillo, J.; Gomperts, R.; Stratmann, R. E.; Yazyev, O.; Austin, A. J.; Cammi, R.; Pomelli, C.; Ochterski, J. W.; Ayala, P. Y.; Morokuma, K.; Voth, G. A.; Salvador, P.; Dannenberg, J. J.; Zakrzewski, V. G.; Dapprich, S.; Daniels, A. D.; Strain, M. C.; Farkas, O.; Malick, D. K.; Rabuck, A. D.; Raghavachari, K.; Foresman, J. B.; Ortiz, J. V.; Cui, Q.; Baboul, A. G.; Clifford, S.; Cioslowski, J.; Stefanov, B. B.; Liu, G.; Liashenko, A.; Piskorz, P.; Komaromi, I.; Martin, R. L.; Fox, D. J.; Keith, T.; Al-Laham, M. A.; Peng, C. Y.; Nanayakkara, A.; Challacombe, M.; Gill, P. M. W.; Johnson, B.; Chen, W.; Wong, M. W.; Gonzalez, C.; Pople, J. A. *Gaussian 03*, 2004; Revision D.01,Gaussian, Inc., Wallingford CT.
24. Sousa, S. F.; Fernandes, P. A.; Ramos, M. J. *J. Phys. Chem. A* **2007**, *111*, 10439.
25. Cossi, M.; Scalmani, G.; Rega, N.; Barone, V. *J. Chem. Phys.* **2002**, *117*, 43.
26. Takano, Y.; Houk, K. N. *J. Chem. Theory Comput.* **2005**, *1*, 70.